Journal of Applied Polymer Science

Optical Density as a Probe of Carbon Nanotubes Dispersion in Polymers

Anthony Combessis,[1,2] Christelle Mazel,[1] Melek Maugin,[1] Lionel Flandin[2]

[1]Nexans Research Center, 29 Rue Pré Gaudry, 69353, Lyon Cedex 07, France

[2]LEPMI UMR 5279 CNRS, Grenoble INP, Univ. de Savoie, Univ. J. Fourier, LMOPS, Bat. IUT, Campus de Savoie Technolac, 73376, Le Bourget Du Lac Cedex, France

Correspondence to: L. Flandin (E-mail: Lionel.Flandin@univ-savoie.fr)

ABSTRACT: The dispersion state of composite materials is known to primarily govern their macroscopic properties. With nanoscopic fillers tiny fluctuations in the interactions among particles may even become the prominent parameter. In this article, the dispersion of carbon nanotubes within a polymer was studied by means of UV–visible spectroscopy and transmitting light microscopy. With thin films, it was found that all the measured absorbances obey a parallel model between the dispersed and the aggregated phases. A method could thus be proposed and validated to gain micrographies of the optical densities within the samples. The Beer–Lambert law was applied to the description of this solid/solid structure, leading to an extinction coefficient for carbon nanotubes comparable to that proposed in solutions. In conclusion, it is shown that one can obtain valuable information from the dispersed phase in optical micrographies, especially the effective filler concentration and a dispersion index in agreement with the literature. © 2013 Wiley Periodicals, Inc. J. Appl. Polym. Sci. 130: 1778–1786, 2013

KEYWORDS: composites; microscopy; morphology; nanotubes; graphene and fullerenes; optical properties

Received 16 November 2012; accepted 25 March 2013; Published online 6 May 2013

DOI: 10.1002/app.39333

INTRODUCTION

Multiscale understanding of polymer composites filled with conductive particles established strong correlations between the electrical properties and the filler geometry,[1,2] content,[3] dispersion state, and distribution.[4,5] By comparison to conventional carbon blacks, carbon nanotubes[6] induce comparable or enhanced electrical or mechanical properties with lowered fractions.[1,7,8] For example, one of the lowest percolation threshold in the literature (0.0025 wt %), was reported several years ago with carbon nanotube filled epoxy composites.[9] However, these very large dilutions make it difficult to measure the effective amount of filler with conventional techniques, like thermogravimetric analysis (TGA). Moreover, controlling the particles arrangement becomes decisive challenge to design materials with controlled and repeatable properties.

Several techniques of morphological characterization can be applied to probe the architecture of composites, from microns to nanometer.[10] Light microscopy (LM) gives information on the dispersion state at micron scale. This common, easy to use, and cost effective technique is usually employed to characterize the shape, size, and density of heterogeneities larger than a few square micrometers. At higher magnification, transmission electron (TEM), scanning electron (SEM), or atomic force microscopies (AFM) are preferred. With a nanometer resolution, these techniques give valuable information on the nanofillers distribution, dispersion state, or orientation but are, consequently, very local probes.

Finally, the overall amount of filler is commonly studied by TGA. Unfortunately, for the very diluted nanocomposites, the resolution of this equipment may not be sufficient.

As carbon nanotubes strongly absorb the visible light, it is possible to determine their concentration in liquid media by means of UV–visible spectroscopy.[11,12] This was shown to obey the Beer–Lambert's law and allowed the determination of extinction coefficient for carbon nanotubes.[13] This article proposes to employ a similar method with light microscopy and on solid–solid systems. Comparison of composites absorbances to their *meso* scale distribution is also discussed.

MATERIALS AND METHODS

Materials

Three series of multiwall carbon nanotubes (MWNT) filled thermoplastic polymers samples were studied. Arkema Graphistrength C100 was used as MWNT. First series, "*K series*," was obtained from successive twin-screw dilutions of a masterbatch in a commercial Very Low Density Polyethylene (VLDPE).

Table I. Carbone Nanotube Loadings and Film Thicknesses for the Samples Used in This Study

K series		*C series*		*sC series*	
MWNT (wt %)	Thickness (μm)	MWNT (wt %)	Thickness (μm)	MWNT (wt %)	Thickness (μm)
0.05	65	0.80	34	0.80	30
0.10	67	1.20	29	1.20	30
0.50	26	1.70	35	1.50	26
1.00	25	2.20	31	2.00	27
2.00	25	2.50	34	2.50	29
3.00	28	2.70	30	5.00	17
4.00	16	5.00	13		
5.00	15				

C and *sC series* were prepared by direct mixing of the MWNT with an ethylene-co-vinyl acetate (EVAc; vinyl acetate content 12 wt %). Fillers were first incorporated into the melt matrix using a 300 cm^3 Brabender mixer for 15 min at 110°C. Composites were then homogenized for 20 min using a two roll mill.

For *sC series*, the MWNT powder was sieved to only retain within the samples the agglomerates smaller than 250 μm. The resulting composite was further processed as described above.

All formulations (Table I) were finally processed by hot melt compression into films with controlled thicknesses decreasing from 65 to 15 μm with increasing the MWNT content.

UV–Visible Measurements

UV–Visible spectroscopy characterizations were performed within the 200–900 nm range (wavelength step: 1 nm, scan speed: 240 nm min^{-1}) using a Perkin Elmer Lambda 11 spectrophotometer.

Light Microscopy

The optical density determination method was developed using a Leica DMLM system microscope in light transmission mode. Sixteen bit grayscale micrographies were acquired with a Leica DFC420 CCD camera using a 5× objective (total magnification 50×) connected to a computer. In this study, all micrographies were performed in a dark room using the whole light spectrum. Camera setup (exposure time, gain, and gamma) and image acquisitions were performed using Leica Application Suite software (LAS v. 2.4.0 R1). Microscope lamp voltage was measured with a Metrix mtx 3281 Multimeter. Optical density calibration was done using Edmund Optics Techspec 63-469 neutral density filters kit (Filters of calibrated optical densities ranging from 0.10 and 3.00; Table II). Micrographies were finally processed using ImageJ freeware[14,15] with the help of in-house codes based on "threshold," "histogram," and "analyze particles" functions.

RESULTS AND DISCUSSIONS

UV–Visible Spectroscopy

To assess the validity of Beer–Lambert's law for our solid–solid systems, MWNT/polymer composites films were observed by means of UV–Visible spectroscopy. The mass extinction coefficient of MWNT (ε_{MWNT}) was then determined from Beer–Lambert's law:

$$A = -\log\left(\frac{I}{I_0}\right) = \varepsilon \times l \times C \quad (1)$$

where A is the absorbance of the system, I_0 and I correspond to the intensities of the incident and transmitted light beams, respectively, l the sample's thickness and C its concentration. ε is the extinction coefficient of the studied filler, here the MWNT.

From the literature, Rance et al.[11] measured MWNT mass extinction coefficient performing UV-Visible spectroscopy on suspended liquid media. These authors concluded that "all values fall within a narrow range from 44.5 to 54.5 mL mg^{-1} cm^{-1} disregarding carbon nanotubes structural parameters."

The UV–Visible response of a series of "*K*" samples is presented in Figure 1. As expected, absorbance increased alongside with the amount of filler. The curves further revealed the presence of a maximum at about 250 nm. This peak was already observed with carbon nanotubes and associated to the electronic delocalization (π-plasmon absorbance).[11,12] At highest volume fractions, the saturation of the measurements did not allow to observe this peak which was however likely to be present.

Mean absorbances within the visible domain (400–800 nm) were studied as function of filler fraction. In order to obtain a comparable data, samples thicknesses were normalized to 15 μm (Figure 2). For ease of comparison, the absorption values of *K*, *C*, and *sC* samples are represented on the same graph.

From the latter, a strong dependency was revealed between the samples preparation and their absorbance. The three different preparations indeed lead to large discrepancies. It was however further noticed that for a given series of samples a linear relationship was evidenced between filler fraction and absorbance. In addition, the slopes obtained with the *K* and *C* series lead to extinction coefficients in agreement with that obtained in the literature for MWNT suspensions (Table III).[11,12]

The differences in slopes could not be ascribed to the composites constituents, because all the MWNT, in this study,

Table II. Optical Density and Transmitted Light (OD = − log *T*) of the Absorptive Neutral Density (ND) Filters Employed for Calibration (Edmund Optics Techspec #63-469 kit)

Optical density	0.10	0.15	0.20	0.30	0.40	0.50	0.60	0.70
Transmittance	79.4%	70.9%	63.1%	50.1%	39.8%	31.6%	25.1%	20.0%
Optical density	0.90	1.00	1.30	1.50	2.00	2.50	3.00	
Transmittance	12.6%	10.0%	5.0%	3.2%	1.0%	0.3%	0.1%	

Applied Polymer SCIENCE

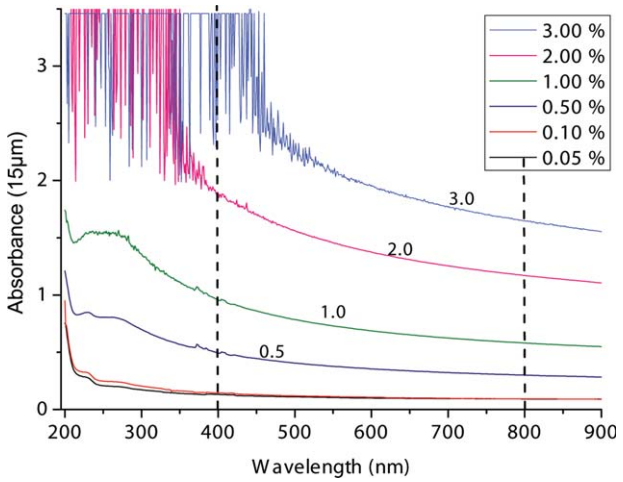

Figure 1. Raw experimental UV–Visible absorbance for *K series* samples as a function of wavelength. Dashed lines delimit the visible domain. The *C* and *sC* (data not shown) presented very similar trends. [Color figure can be viewed in the online issue, which is available at wileyonlinelibrary.com.]

originated from the same batch. The polymeric host, with a very small absorption coefficient as compared to the MWNT was not likely either to be responsible for the differences. Because the measurements in solution have to be made with high dispersion quality, it was assumed that partial aggregation could induce variations. It was thus decided to perform light microscopy measurements to assess the quality of the dispersion within the different samples.

Light Microscopy

Light microscopy (LM) is a simple, fast, and cost effective tool widely used to characterize the dispersion of the carbon nanotube within the polymeric host.[16,17] A typical photomicrograph of these materials can generally be segmented in two domains. The *foreground* includes large heterogeneities. It is constituted by the darker areas and related to non-dispersed carbon nanotubes. The number of aggregates per surface unit, together with their geometric properties (e.g., shape ratio, area, and perimeter), are commonly employed to estimate the filler dispersion at micron scale. Several dispersion indexes have been proposed to that purpose.[17,18] Regarding the electrical properties and percolating network construction, aggregates represent an unfavorable phase with high concentration of carbon nanotubes essentially wasted.

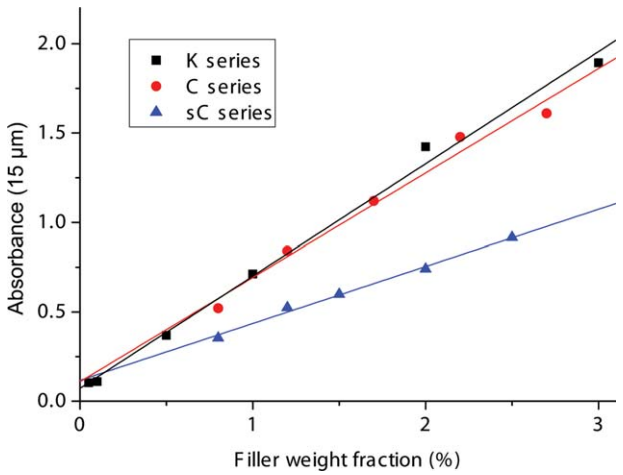

Figure 2. Effect of the filler concentration (wt %) on the absorbance for the three series of samples. These $A_{15\mu m}$ values were defined as the mean absorbance of a 15 µm sample in the 400–800 nm wavelength range. [Color figure can be viewed in the online issue, which is available at wileyonlinelibrary.com.]

Table III. Measured Extinction Coefficients for the Three Series of Samples: with the Same Type of Carbon Nanotube, the Measured Absorbance is Significantly Altered by the Preparation Method

Series	Slope of $A_{15\mu m}$ versus V_f	Overall extinction coefficient (mL $mg^{-1}.cm^{-1}$)
K	0.628	41.9 ± 0.8
C	0.584	38.9 ± 0.8
sC	0.318	21.3 ± 0.5

The *background* of micrographies is generally not considered or observed at higher magnification (AFM, TEM, …), although this phase—made of objects not distinguishable at light microscopy observation scale—is likely to contain information on submicronic fillers. Moreover, this phase is continue and must therefore govern the electrical properties of composites. Albeit it depends on parameters such as the sample's thickness and the observation settings, the grey level observed on light micrographies should give hint on the amount of filler at sub-micron scale.

Estimation of the Dispersion Indexes

The dispersion quality of the samples was evaluated by means of transmitting light microscopy. Dispersion indexes were calculated from the following equation given in the literature:[17]

$$D = \left(1 - f \times \frac{\frac{S_{CNT}}{S_0}}{\varphi_{vol}}\right) \times 100 \quad (2)$$

where S_{CNT} is the area occupied by MWNT aggregates with areas larger than 5 μm^2 ; S_0 the total picture area ; Φ_{vol} carbon nanotube volume fraction and f a constant factor that describes the aggregates density (estimated to be equal to 0.25).[17,19] If D = 100% the dispersion state is considered as being perfect at the observation scale.

The dispersion indexes versus filler weight fractions for *K*, *C*, and *sC* series are presented in Figure 3. Distinct behaviors are observed, in agreement with the hypothesis that the experimental extinction coefficient primarily depend on the dispersion state of MWNT. On one hand, *K series* was prepared by successive dilutions of a masterbatch and scores a 94% mean dispersion index. Dispersion indexes are very similar for all samples. In other words, this series appears almost fully dispersed at micron scale. Correlation of this result to the measured extinction coefficient—which fell in a very close range of the literature values—tends to confirm that UV–Visible determination of fillers extinction coefficients in solid–solid systems requires fully dispersed samples at the observation scale.

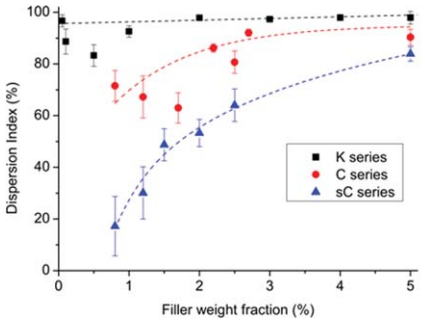

Series	<D>
K series	94%
C series	79%
sC series	49%

Figure 3. Dispersion indexes versus filler concentration for the three series of samples, the dashed lines are eyes guidelines. [Color figure can be viewed in the online issue, which is available at wileyonlinelibrary.com.]

In contrast to both *sC* and *C series*, processed by direct mixing of MWNT with the polymer, show increasing dispersion index with filler fraction. From the lowest to the highest filler concentration, *D* increased by 60% and 25% for the for "*sC*" and "*C*" samples, respectively. This can originate from the amplified filler to filler interactions responsible for agglomerates breakup during the mixing process. Aggregates fragmentation and erosion mechanisms[17,20] are indeed more likely to occur in more concentrated systems. On the application standpoint, this means that the use of carbon nanotube masterbatches dispersed in polymers is not only preferable for practical reason, but should also be preferred to improve the micron-scale dispersions.

Optical Density by Light Microscopy

In a transmission mode, light microscopes measure the intensity of light that could pass through the observed samples. Dark areas thus correspond to the zones where the light from the source is more efficiently absorbed by the sample. This is very similar to a numerical spectrophotometer. A grey level picture actually represents a quantification of the amount of transmitted light on a given position. Besides the spatial resolution, light microscopes differ from regular spectrometers because the latter are regularly calibrated prior to measurements, and use monochromatic sources. A specific methodology was therefore developed to calibrate the measurements with light microscopy and validate the technique with polychromatic sources.

Using light microscopy, a series of images was obtained in the form of 16 bit grayscale. The grey levels appeared correlated to several parameters for which individual contributions had to be identified:

- incident light intensity;
- CCD detector response, controlled by gamma, gain, and exposure time parameters;
- sample's transmittance (T), that depends on composition and geometry.

The individual influences of the microscope parameters were first studied with the help of calibrated filters in order to define and validate a "microscope law" for determination of optical density. For easy differentiation from UV–Visible spectroscopy, polychromatic absorbance measurements performed by means of light microscopy are named "optical density" (OD) in this study.

Determination of the Microscope Law

Incident Light Intensity. For incandescent lamps, the luminous intensity and the applied voltage are inter related by a power-law relationship[21]: $I \propto V_\gamma$. Thus, an indirect but reliable and easy way to control the incident light intensity is to measure the voltage applied to the microscope lamp. This voltage–intensity relationship was experimentally verified many times with our system configuration, Figure 4(a). A value of $\gamma = 3.85 \pm 0.05$ was obtained.

Response of CCD Detector. The transmitted light intensity has to be calculated from the numeric photomicrograph. Light microscopy may obviously not reveal the individual MWNT, but the mean grey level of the background is likely to indicate the

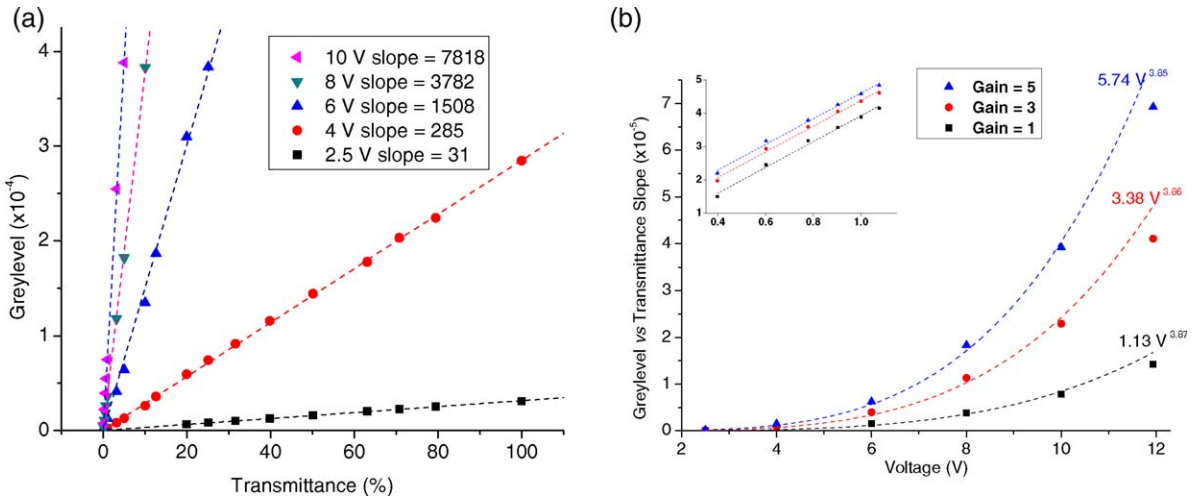

Figure 4. Determination of Voltage Exponent γ in the microscope law equation [eq. ((3))]. (a) Grey level versus transmittance for several voltages: the slope in this plot increases with the light source beam intensity as the corresponding micrograph becomes lighter. (b) Influence of the applied voltage on the measured grey levels for three values of the gain. Inset shows the logarithmic plot to determine the κ parameter ($\gamma = 3.85 \pm 0.05$). [Color figure can be viewed in the online issue, which is available at wileyonlinelibrary.com.]

Parameter	Value	Error
K	0.115	21.7%
α	1.0	1.0%
ι	1.0	0.9%
τ	1.0	0.6%
κ	3.85	3.7%

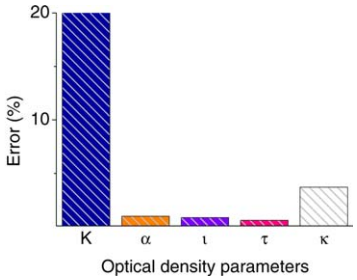

Figure 5. Final set of parameters for the calibration of the light microscope to measure optical densities. (Only β and γ are supposed to be dependent on the experimental setup.) [Color figure can be viewed in the online issue, which is available at wileyonlinelibrary.com.]

amount of MWNT dispersed in the polymer. Practically, the CCD detector response is altered by tuning gamma, gain, or exposure time. This naturally impacts grey levels. Because our experiments did not require changing the gamma parameter, the latter was fixed to unity. Increasing the exposure time or gain tends to lighten the photomicrograph and to increase the grey levels to higher (whiter) values. Grey levels (GL) were thus expected to take the following form:

$$\mathrm{GL}=\beta\times T^{\alpha}\times \mathrm{Gain}^{\iota}\times \mathrm{Voltage}^{\gamma}\times \mathrm{Time}^{\tau} \quad (3)$$

where β is a constant related to the specific device and therefore called *microscope calibration constant*. It takes into account the microscope's light path, from light source to CCD detector, the lamp characteristics and all the structural features of the device. The α exponent value was experimentally determined plotting Log(GL) versus Log(T). ι, γ, and τ exponents correspond to slopes in *Log* (GL vs. T slope) versus Log(Gain), Log(Voltage), and Log(Time) respectively [Figure 4(b)]. The mean value of β was calculated by minimizing the square error between calculated and experimental GL values for 30 experiments with

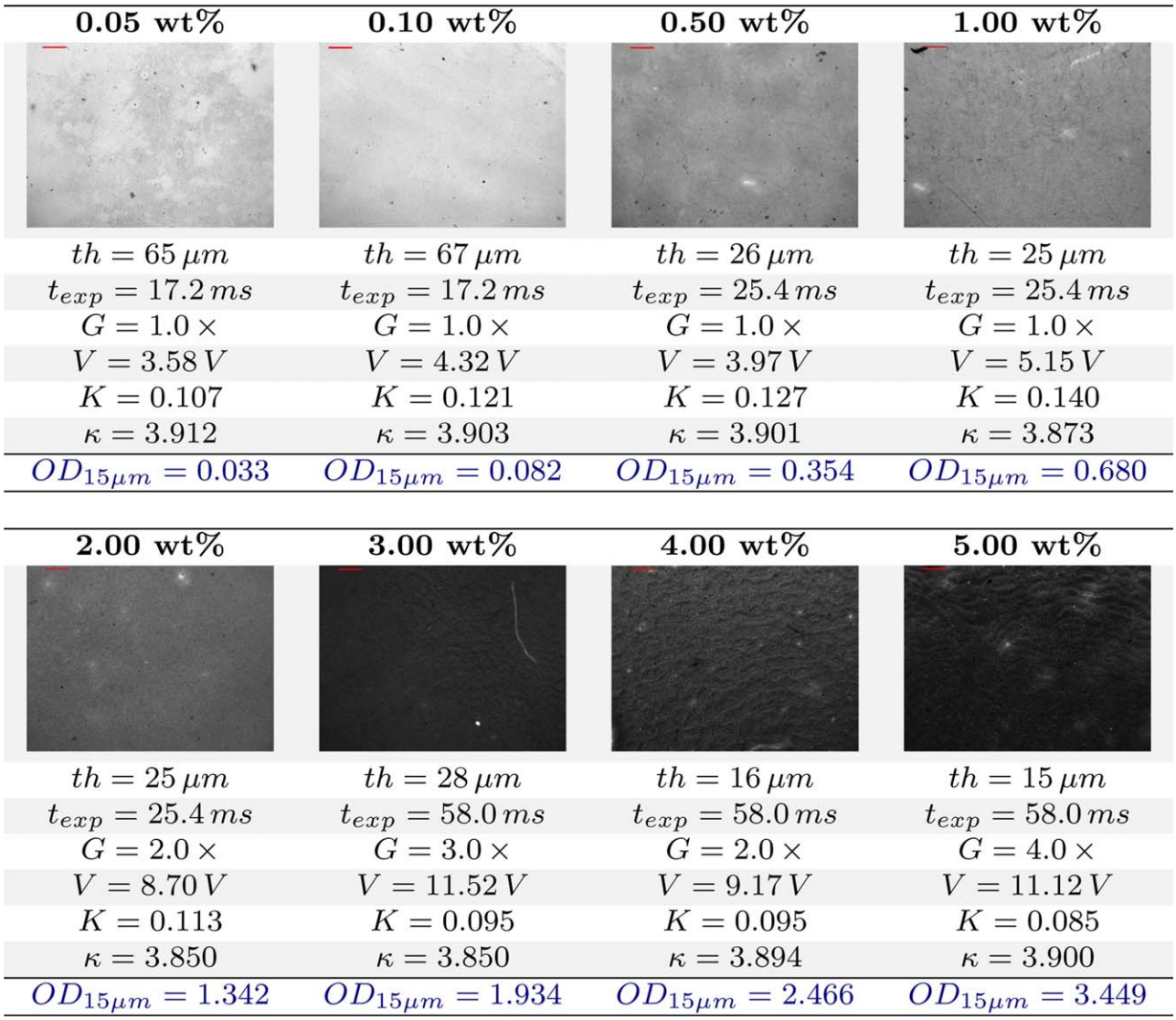

Figure 6. Typical photomicrographs for various films, amounts of filler and films' thicknesses. Chosen experimental conditions to obtain the pictures. Resulting optical densities after correction of the experimental features. The scale bar represents 250 μm in length. (The dispersion state is not considered here.) [Color figure can be viewed in the online issue, which is available at wileyonlinelibrary.com.]

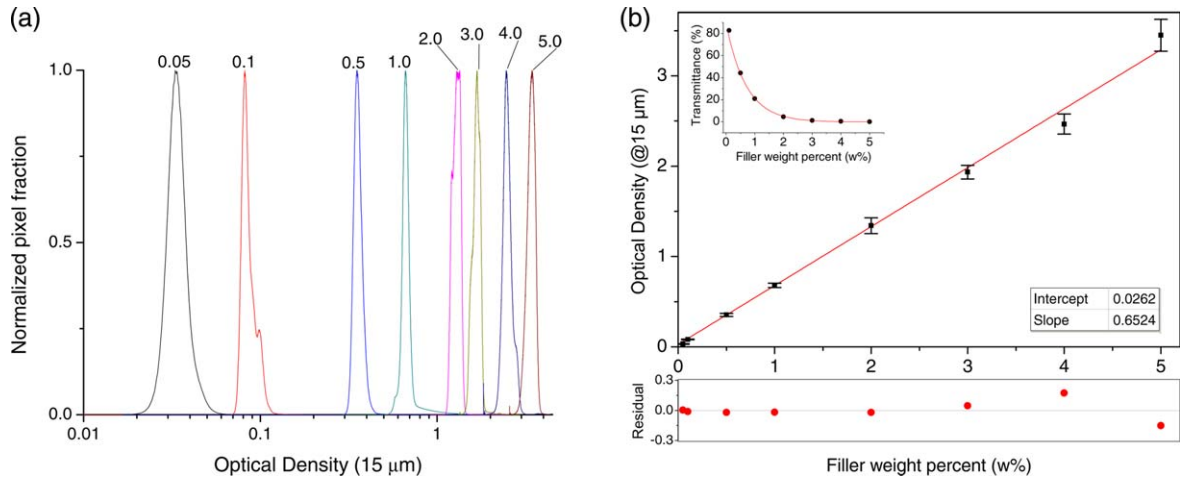

Figure 7. Application of the experimental technique to determine the Optical Density (OD) of unknown samples. (a) Optical densities of several carbon nanotube/PE nanocomposites, the weight percent in MWNT for each sample is indicated on the top of the graph ($n = 10$). (b) Effect of filler concentration on the OD at 15 µm. (The corresponding transmittance variation are shown in the inset.) The error bars here correspond to the width of the optical density's peak measured for 10 samples (at 0.63 of the peaks' heights). [Color figure can be viewed in the online issue, which is available at wileyonlinelibrary.com.]

calibrated filters. The resulting set of parameters and standard errors are collected and plotted in Figure 5.

The results indicate that α, ι, and τ mainly correspond to the CCD behavior and followed the expected trends with very good stability over time and low sensibility to the nature of the samples. These three parameters were thus considered constant and equal to one. In contrast, β and γ presented much larger uncertainties and should thus be regarded with more attention. For best precision on optical density measurement, a new calibration was performed on a daily basis to accurately determine β and γ values. The calibration requires testing at least three neutral density filters within the expected range of the samples to be measured, prior to any testing of unknown samples.

Finally, the microscope's law for optical density determination takes the form:

$$\mathrm{OD} = -\log(T) = -\log \frac{\mathrm{GL}}{100 \times \beta \times \mathrm{Gain} \times \mathrm{Voltage}^{\gamma} \times \mathrm{Time}} \qquad (4)$$

Effect of Samples Thickness. According to Beer–Lambert's law, a proportional relationship is expected between the optical density of a sample and its thickness. In order to compare samples with various thicknesses, the following normalization was performed:

$$\mathrm{OD}_{\mathrm{norm}} = \frac{\mathrm{Normalization\ \ Value}}{\mathrm{Sample\ \ Thickness}} \times \mathrm{OD} \qquad (5)$$

Characterizing Composites with Optical Density

The validation of a microscope calibration law made it possible to measure and compare optical densities of various samples measured in very dissimilar manners. It was more specifically used to compare the dispersed phase of samples presenting different thicknesses, and filler concentrations. The observation parameters had indeed to be largely varied depending on the specimen absorbencies.

First, optical densities of *K series* composites, with the best dispersion index and a homogeneous appearance in the light microscopy, were measured and compared to UV–Visible absorbencies for validation. The *sC* and *C* composites were then studied the same way.

Figure 6 summarizes samples information and observation parameters for *K series*. The best fit values for β and γ are reported as well as the resulting optical densities.

The impact of the nominal weight fraction of filler on the measured optical densities is presented in Figure 7. Figure 7(a) shows the normalized pixel fractions as a function of the grey levels converted into optical density. Each curve represents the average value of at least 10 micrographies with a given amount of filler. Each presents a very well-defined peak with an easy to determine maximum that was considered as the optical densities of the considered films. In Figure 7(b) is plotted 15 µm optical density versus filler weight fraction (V_f). A linear relationship is evidenced between optical density and filler concentration, meaning that the data obtained from light microscopy are in excellent agreement with the Beer–Lambert's law. Only for the darkest films was the difference between the experiment and the model a bit larger.

To further validate this appealing method, optical densities measured by light microscopy were compared to UV–Visible spectroscopy absorbances. For all three series, OD values—obtained using a white polychromatic halogen lamp—are found close to mean absorbances, calculated within the visible domain (400 – 800 nm; Figure 8). This method furnished results very comparable to those of the UV–Visible measurements. The three kind of samples indeed presented a linear behavior, but with significantly different slopes in OD versus V_f. In other words, all type of samples followed the Beer–Lambert law but with different extinction

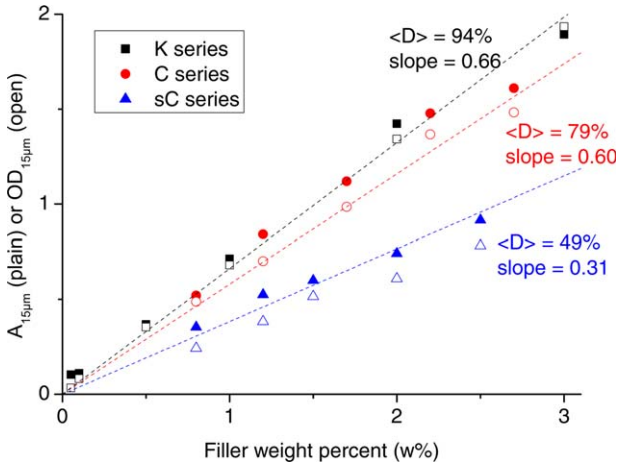

Figure 8. Comparison of microscopic optical densities (open) with the spectrophotometric absorbances (plain). $A_{15\mu m}$ are mean values calculated within the 400–800 nm Range. ODs are in agreement with $<A>$. The three systems under study exhibit a linear behavior, although the slope increases with the mean dispersion index measured by LM. [Color figure can be viewed in the online issue, which is available at wileyonlinelibrary.com.]

coefficients. This seemed incorrect, because the extinction coefficient is supposed to be an intrinsic properties and all MWNT were obtained from the same batch. A detailed analysis of the uncertainty revealed that the differences could neither originate from OD measurements nor from the estimations of the samples thicknesses. The differences in OD versus V_f should be related to the effective filler fraction. In summary, optical density and UV–visible techniques seem to be largely impacted by the effective filler concentration of the dispersed phase.

The dispersion indexes (D; Figure 9) indicate that the poorer the dispersion, the lower the effective ε value. This can be attributed to the fact that lower D reveals the presence of more numerous or bigger aggregates of MWNT that do not contribute to darken the dispersed phase. If this is correct, the MWNT mass extinction coefficient should correspond to OD/V_f for perfectly dispersed system. Because D index of *K series* is close to 100%, the actual value for should be close to $\varepsilon K = 43.3 \pm 0.3$ mL mg^{-1} cm^{-1}.

In Figure 10(a) linear relationship is evidenced between (OD/V_f) and mean dispersion indexes. The extrapolation of mass extinction coefficient value for fully dispersed systems leads to . Through film thickness, the optical density of composites seems to obey a parallel model between aggregated and dispersed phases. This model assumes that the aggregation process lowers the overall optical density by reducing the volume fraction of carbon nanotubes in the dispersed phase (ε_{eff}):

$$OD = (\varepsilon \times l \times C)_{eff} = \frac{\varepsilon_{disp} \times l \times \varphi_{eff}}{1 - \frac{S_{CNT}}{S_0}}; \quad \varphi_{eff} = \frac{V_f \times D}{1 - \frac{S_{CNT}}{S_0}} \qquad (6)$$

This could be simplified to get a straightforward and accurate approximation of the parallel model:

$$OD \approx \varepsilon_{MWNT} \times l \times V_f \times D \qquad (7)$$

In addition to expressing the meaning of the dispersion coefficient, this approach also rationalizes the agreement between UV–Visible and light microscopy measurements. For each of the 21 considered formulations, calculated OD values from the latter equation were compared to the measured ones (Figure 10). ε_{MWNT} = 47.2mL mg^{-1} cm^{-1} was taken as MWNT mass extinction coefficient. Very good agreement was observed between calculated and measured optical densities, after correction of the dispersion index.

Least squares method was finally applied to OD_{calc} versus OD_{meas} residual to determine the mass extinction coefficient of MWNT with enhanced accuracy. A value of ε_{MWNT} = 47.0 mL mg^{-1} cm^{-1} was obtained.

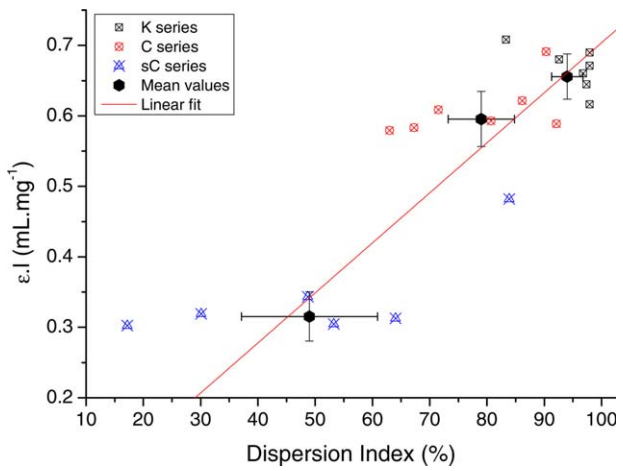

Figure 9. Interrelationship between the Beer–Lambert parameter (εl) and the mean dispersion index (measured with LM). The scatter at D close to 49 and 79% indicates significant variations in the filler contents in these systems. [Color figure can be viewed in the online issue, which is available at wileyonlinelibrary.com.]

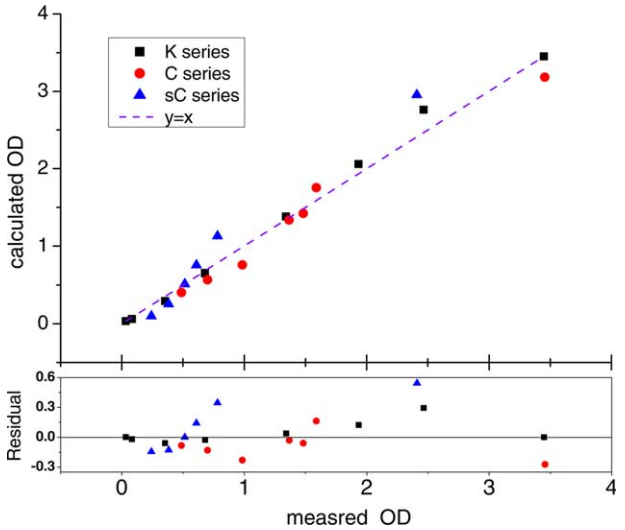

Figure 10. Validation of the optical densities (OD) analytical approximation by comparison of the experimental measurements with the calculations ($OD \approx \varepsilon_{MWNT} \times l \times V_f \times D$) with no adjustable parameter. [Color figure can be viewed in the online issue, which is available at wileyonlinelibrary.com.]

Table IV. Total (V_f) and Dispersed (V_d) Filler Weight Fractions for the Studied Composites Calculated From Samples Effective Mass Extinction Coefficients [ε (mL mg^{-1} cm^{-1})] Assuming a Parallel Model of the Dispersed and Agglomerated Phases

K Series			*C Series*			*sC Series*		
ε_{eff} (mL mg^{-1} cm^{-1})	V_f (wt %)	V_d (wt %)	ε_{eff} (mL mg^{-1} cm^{-1})	V_f (wt %)	V_d (wt %)	ε_{eff} (mL mg^{-1} cm^{-1})	V_f (wt %)	V_d (wt %)
44.0	0.05	0.046	40.6	0.80	0.69	20.2	0.80	0.34
54.7	0.10	0.12	38.9	1.20	0.99	21.3	1.20	0.54
47.2	0.50	0.50	38.6	1.70	1.39	22.9	1.50	0.73
45.3	1.00	0.96	41.4	2.20	1.93	20.3	2.00	0.86
44.7	2.00	1.89	39.5	2.50	2.09	20.9	2.50	1.10
43.0	3.00	2.72	39.2	2.70	2.24	32.1	5.00	3.39
41.1	4.00	3.47	46.1	5.00	4.61	-	-	-
46.0	5.00	4.86	-	-	-	-	-	-

A significant advantage the presented technique is that the effective dispersed phase filler concentration V_d can easily be deduced from OD measurements and ε_{MWNT}. This makes optical density determination by light microscopy technique complementary to TGA (Table IV).

CONCLUSIONS

Meso–macro relationships in MWNT/polymer composites were studied by means of light microscopy approach where the aggregated and dispersed phases were assessed.

The large heterogeneities were probed by dispersion indexes determination. The value proposed in the literature for the density of the aggregate ($f = 0.25$)[19] was found in excellent agreement with the set of results from this study.

A technique to probe the dispersed phase by means of light microscopy was developed. The measured optical densities were shown to be similar to mean absorbance values obtained performing UV–Visible spectroscopy within the visible wavelengths range. OD measurements allowed the accurate determination of MWNT extinction coefficient on solid–solid systems. A value of 47.0 mL mg^{-1} cm^{-1} was obtained.

Because optical densities, UV–Visible absorbances and dispersion indexes are related to the dispersed and total volume fractions of filler, it is thus possible to switch from each other.

- Using carbon nanotube extinction coefficient, light transmission microscopy, as well as UV–Visible spectroscopy, can be employed to determine the effective dispersed phase concentration V_d, making both techniques complementary to TGA.
- Comparing (OD vs. V_f) or (A vs. V_f) slopes to $\varepsilon_{MWNT}.l$ samples dispersion indexes can be determined. In other words, it is possible to assess samples micron-scale dispersion quality with spectroscopic experiments.
- Starting from dispersion index and V_f, it is possible to get an estimation of the dispersed phase concentration V_d. The obtained value would however be less accurate than with optical density, principally for two reasons: (i) dispersion index calculation requires in such cases to take into account aggregates sizes within the range of technique's observation resolution, implying image processing counting errors; (ii) carbon nanotube aggregates density is unknown, not accessible with this characterization and has to be estimated.[19,22]

The sub-micron observation scale available with optical density ranks the proposed technique between light microscopy and transmission electron microscopy (TEM). Another advantage of the latter is to prevent microstructure modifications or degradations that could occur during TEM observations.

The optical density technique could easily be applied to other composite systems such as carbon black filled materials. An example of application has also been recently proposed with fullerene based composites for photovoltaic applications.[23] It could also be implemented for the quality control of compounds, and even to follow online processes. Another possible application concerns metal coating thickness measurement or permeability assessment[24] on metal coated polymer films.

ACKNOWLEDGMENTS

We acknowledge our colleagues from Arkema-GRL for providing MWNT powders and masterbatch. Special thank to X. Festaz from Nexans Research Center who extruded *K series* samples. The financial support of OSEO through the Genesis grant is acknowledged.

REFERENCES

1. Nan, C. W. *Prog. Mater. Sci.* **1993**, *37*, 1.
2. Carmona, F. *Phys. A* **1989**, *157*, 461.
3. Kirkpatrick, S. *Rev. Mod. Phys.* **1973**, *45*, 574.
4. Manas-Zloczower, I. *Rheol. Bull.* **1997**, *66*, 229.
5. Schadler, L. S. Polymer-based and polymer-filled nanocomposites. In Nanocomposite Science and Technology, Ajayan, P. M., Schadler, L. S., Braun, P. V. Eds.; Wiley-VCH Verlag GmbH & Co. KGaA: Weinheim, **2004**; pp 77–153.
6. Iijima, S. *Nature* **1991**, *354*, 56.

7. Celzard, A.; McRae, E.; Deleuze, C.; Dufort, M.; Furdin, G.; Marêché, J. F. *Phys. Rev. B* **1996**, *53*, 6209.
8. Foygel, M.; Morris, R. D.; Anez, D.; French, S.; Sobolev, V. L. *Phys. Rev. B* **2005**, *71*, 104201.
9. Martin, C. A.; Sandler, J. K. W.; Shaffer, M. S. P.; Schwarz, M.-K. Bauhofer, W.; Schulte, K.; Windle, A. H. *Compos. Sci. Technol.* **2004**, *64*, 2309.
10. Pegel, S.; Villmow, T.; Pötschke, P. In Polymer-Carbon Nanotube Composites: Preparation, Properties and Applications; McNally, T., Pötschke, P. Eds.; . Woodhead Publishing: Cambridge, **2011**; pp 265–294.
11. Rance, G. A.; Marsh, D. H.; Nicholas, R. J.; Khlobystov, A. N. *Chem. Phys. Lett.* **2010**, *493*, 19.
12. Jeong, S. H.; Kim, K. K.; Jeong, S. J.; An, K. H.; Lee, S. H.; Lee, Y. H. *Synth. Methods* **2007**, *157*, 570.
13. Smith, J. G., Jr.; Connell, J. W.; Watson, K. A.; Danehy, P. M. *Polymer* **2005**, *46*, 2276.
14. Abramoff, M. D.; Magelhaes, P. J.; Ram, S. J. *Biophoton. Int.* **2004**, *11*, 36.
15. Rasband, W. S. ImageJ. US National Institutes of Health, Bethesda, MD, http://rsb.info.nih.gov/ij/, 1997–2009.
16. Leer, C.; Carneiro, O. S.; Covas, J. A.; Maia, J. M.; van Hattum, F. W. J.; Bernardo, C. A.; Biro, L. P.; Horvath, Z. E.; Kiricsi, I. *Mater. Sci. Forum* **2006**, 514–516, 1125.
17. Villmow, T.; Pötschke, P.; Pegel, S.; Häussler, L.; Kretzschmar, B. *Polymer* **2008**, *49*, 3500.
18. Leblanc, J. L.; Putman, M.; Pianhanuruk, E. *J. Appl. Polym. Sci.* **2011**, *121*, 1096.
19. Le, H. H.; Kasaliwal, G.; Ilisch, S. *Kautsch. Gummi Kunstst.* **2009**, *06*, 326.
20. Kasaliwal, G. R.; Pegel, S.; Göldel, A.; Pötschke, P.; Heinrich, G. *Polymer* **2010**, *51*, 2708.
21. Fink, D. G.; Beaty, H. W. Standard Handbook for Electrical Engineers, 11th ed.; McGraw-Hill: New York, **1978**.
22. Medalia, A. I. *J. Colloid Interface Sci.* **1970**, *32*, 115 .
23. Nourdine, A.; Perrin, L.; de Bettignies, R.; Guillerez, S.; Flandin, L.; Alberola, N.. *Polymer* **2011**, *52*, 6066.
24. Garnier, G.; Brechet, Y.; Flandin, L. *J. Mater. Sci.* **2009**, *44*, 4692.